Journal of Molecular Biology and Molecular Imaging

Open Access

Austin Publishing Group

Research Article

Chemical Imaging by NanoSIMS Provides High-Resolution Localization of the G-Quadruplex Interactive Drug (Br)-PhenDC3 on Human Chromosomes

Verga D[1,2], Hamon F[1,2,3], Nicoleau C[4], Guetta C[1,2], Wu TD[1,2], Guerquin-Kern JL[1,2], Marco S[1,2]* and Teulade-Fichou MP[1,2]*

[1]Institut Curie, PSL Research University, CNRS, UMR9187, F-91405 Orsay, France

[2]INSERM, U1196, Université Paris Sud, Université Paris-Saclay, F-91405 Orsay, France

[3]Curium, RN306, 91400 Saclay, France

[4]Ipsen Innovation, 5 Avenue du Canada, 91140 Les Ulis, France

***Corresponding author:** Teulade-Fichou MP, Institut Curie-Campus Universitaire d'Orsay, Rue Becquerel. Bat 110, 91405 Orsay Cedex, France

Marco S, Institut Curie-Campus Universitaire d'Orsay, Rue Becquerel, Bat 110, 91405 Orsay Cedex, France

Received: June 28, 2017; **Accepted:** July 20, 2017; **Published:** July 27, 2017

Abstract

Determining the distribution of biologically active compounds within cells is a major issue to understand their mechanism of action and to optimize their properties. Over the past decade DNA secondary structures called G-quadruplexes (G4) have been identified as key modulators of genomic functions. This very active research field has led to the development of G4-targeted molecular probes that are used to track quadruplex forming domains in cells, which is achieved, in most cases, by conventional fluorescence microcopy. However, the intrinsic low resolution of fluorescence microcopy as well as the necessity to tag the drugs with fluorophores represent strong limitations. Here we present the use of secondary ion mass spectroscopy imaging (nanoSIMS) for mapping within metaphase human chromosomes the distribution of a bromo-bisquinolinium phenanthroline derivative (Br- PhenDC3) used as G-quadruplex probe. In addition a statistical approach to increase the accuracy and the spatial resolution of the nanoSIMS imaging was implemented as a plug in for the image analysis software ImageJ. The results demonstrate the presence of Br-PhenDC3both at terminal and interstitial regions of chromosomes and constitute a demonstration of the effectiveness of nanoSIMS imaging as an alternative method for accurate genome-wide mapping of DNA interactive drugs.

Keywords: Chemical imaging; Secondary ion mass spectroscopy imaging; NanoSIMS; DNA binding molecules; G-quadruplexes

Introduction

Most anticancer chemotherapeutic agents used in the clinic as frontline drugs act as nuclear DNA binders. These agents are considered to bind more or less randomly on the polymeric structure of DNA, or at least in a non-controllable manner thereby hitting both crucial target regions and off-target regions. This uncontrollable distribution is assumed to be responsible for the high cytotoxicity and the potential mutagenicity frequently associated with DNA interactive drugs, two features often used as decisive arguments to decrease research and development studies on this class of compounds. Therefore, determining whether DNA drugs localize uniformly or show preference for certain genomic regions has become a crucial issue for the development of optimized DNA binding anticancer agents in the future. Surprisingly this topic remains largely unexplored so far, essentially due to the lack of genome-wide analytical methods. However this has been recently challenged by the emergence of Chemical-Sequencing (Chem-Seq) methodologies which propose to map the genomic distribution of drugs by identifying drug-induced DNA damages or repair protein recruitment using chemical capture and sequencing [1-4]. Nevertheless, although powerful and highly promising, Chem-Seq approaches are still technically challenging, highly expensive in the case of whole-genome studies and require extreme caution in data analysis with stringent bioinformatics procedures [5,6]. In addition, they provide indirect read out and not direct visualization of drug DNA binding targets. Consequently, there is a strong need for new complementary imaging methods for identifying the distribution of DNA interactive drugs at the genomic level.

Although drugs can be labelled with fluorescent tags (or be intrinsically fluorescent) routine fluorescence microscopy provides resolution limited by light diffraction thereby enabling only the detection of spots (foci) corresponding to the presence of at least 20-40 fluorophores or more. This works fine for immunostaining strategies, in which the fluorescent signal is amplified by heavily labelled antibodies, but it is not applicable to the detection of small molecules unless these are confined in sub compartments (e.g. nucleus, mitochondria, lysosomes),which increases the density of fluorescent markers. Moreover, the labelling of drugs represents an issue as most fluorophores impact target recognition and may modify drug intracellular localization and penetration [7-9]. Although super resolution microscopies hold great potential for chromosome and cellular imaging with high spatial resolution, they are far from being routine imaging techniques and they are highly dependent on the specific photophysics of the dyes.

For two decades we have been involved in the design of drugs targeting DNA secondary structures called G-quadruplexes (G4). These tetra helical structures arise in sequences containing repeat of guanine stretches that fold over due to self-assembly of guanine bases into quartets. It is now well documented that G4s exist in a conformational equilibrium with single-stranded DNA

Citation: Verga D, Hamon F, Nicoleau C, Guetta C, Wu TD, Guerquin-Kern JL, et al. Chemical Imaging by NanoSIMS Provides High-Resolution Localization of the G-Quadruplex Interactive Drug (Br)-PhenDC3 on Human Chromosomes. J Mol Biol & Mol Imaging. 2017; 4(1): 1029.

domains transiently generated during major DNA transactions like replication, transcription, repair and recombination [10], which make them potential roadblocks for the enzymatic machineries operating these vital processes.G4s constitute privileged receptors for small molecules thereby offering possibility to achieve structure-targeted pharmacological action. Therefore, G4 interactive small molecules (G4-ligands) represent a new class of DNA drugs differing from the classical ones as they are assumed to act region selectively at specific genomic G-rich loci such as telomeres, oncogene promoters, tandem mini satellites that are more likely to generate quadruplexes [11]. Interestingly quadruplex-targeted agents, in most cases, do not display acute cytotoxicity and constitute new promising anticancer drugs, which is currently a topic of considerable interest [12-16]. G4 ligands may display various cellular phenotypes, which are attributed to the targeting of different G4s with various accessibilities within G-rich domains. It would be therefore of great interest to map the genomic binding sites of G4 ligands to gain understanding and better define their therapeutic potential. In terms of imaging, a crucial consideration is that genome-wide mapping of drugs cannot be achieved with significant spatial resolution in the context of chromatin due to complex 3D architecture, thus an alternative approach is to operate at the level of metaphase chromosomes.

Herein we report on the use of NanoSIMS (nanoscale Secondary ion Mass Spectrometry) chemical imaging technique for accurate localization of the quadruplex DNA probe PhenDC3 at the level of human chromosomes. PhenDC3 is a bisquinolinium phenanthroline derivative considered one of the best benchmark G4-ligand sticking to most G4 targets with nano molar Kd and featuring low to no binding to other DNA conformations [17]. This compound therefore represents a robust G4 reporter that has been validated in many *in vitro* and in-cell functional studies [18-20].

NanoSIMS is based on a focused energetic primary ion beam (in general Cs^+ or O^-) that is directed onto the sample surface which triggers a collision cascade and generates emission of secondary ion particles. Representing the surface composition, the secondary ions are then collected and guided to a mass spectrometer, which sorts the different ions according to their mass-to-charge ratio. At the exit of the spectrometer, a set of detectors record in parallel the intensity of ions corresponding to different preselected masses from the same micro-volume. By scanning the probe across the sample surface, a chemical map of the sample can then be generated, providing elemental and isotopic information [21,22].

The high detection efficiency of SIMS technique for halogens (I, Br, Cl, F) allows their detection simultaneously to main elements present in biological samples (C, N, S, P). This feature exhibits strong advantage for tagging drugs using halogens at low labeling level as compared to radio labeling as they are easy to introduce, highly chemically stable and in most cases do not affect the drug target recognition. Indeed halogen introduction on drugs is a classical practice of medicinal chemistry to modulate electro negativity of aromatic rings and to improve hydrophobicity. Therefore, for the purpose of the present study, we introduced a bromine atom at position 5 on the phenanthroline core of PhenDC3, to obtain a suitable compound (Br-PhenDC3) able to act as reporter for NanoSIMS chemical imaging.

Materials and Methods

Synthesis of Br-PhenDC3 and evaluation of its biophysical properties compared to PhenDC3

PhenDC3 has been brominated at position 5 on the phenanthroline core as this position is easy to functionalize following a standard protocol and is not likely to affect the binding to G4 targets (Supplementary information Figure 1). FRET-melting assay was performed in 96-well plates on real time PCR apparatus 7900HT Fast Real-Time PCR System as follow: 5min at 25°C, then increase of 0.5°C every minute until 95°C. Each experimental condition was tested in duplicated in a volume of 25µL for each sample. FRET-melting assay was performed with oligonucleotides that mimic the human telomeric sequence, as well as other quadruplex-forming oligonucleotides, equipped with FRET partners at each extremity. The oligonucleotides were prepared at 0.2µM, the ligands at 1µM and competitors at 3 and 10µM final concentration. Measurements were made with excitation at 492nm and detection at 516nm in a buffer of lithium cacodylate (10mM, pH 7.2), KCl (10mM, completed by 90mM LiCl for F21T, and 1mM, completed by 99mM LiCl for all the others G-quadruplex sequences) then heated at 95°C for 5min and left to cool down at 4°C overnight. The employed sequences are:

F21T[6FAM-GGGTTAGGGTTAGGGTTAGGG-3TAMRA],

FCEB25wtT[FAM-AAGGGTGGGTGTAAGTGTGGGTGGGT-TAMRA],

FCEB25-L121T[FAM-AAGGGTGGGTTGGGTGGGT-TAMRA], and

FPu24TT[FAM-TGAGGGTGGTGAGGGTGGGGAAGG-TAMRA]

with FAM: 6-carboxyfluorescein and TAMRA: 6-carboxy-tetramethylrhodamine).

Competition experiments where performed in the presence of duplex DNA:

ds26[CAATCGGATCGAATTCGATCCGATTG]

Cell culture and drug treatment

The human embryonic kidney cells 293 (HEK-293)was grown in RPMI medium completed by 2mM of glutamine, 0.1mg/mL of streptomycin, 100U of penicillin and 10% of fetal bovine serum (Gibco). Cells were treated with 0.3µM of Br-PhenDC3 at 37°C under humidity and 5% CO_2 conditions for 48h. Cellular growth was quantified using the particle counter Z2 Coulter® (Beckman, COULTER®).

Chromosome spreads

Metaphase chromosome spreads were performed following a protocol previously reported [23]. HEK-293 was cultured in the same conditions mentioned above. Cells were then incubated with colchicine (1µg/ml, Eurobio) at 37°C for 90min. After washing, trypsinisation (trypsin–EDTA 0.05% (Eurobio)) and centrifugation (1500 r.p.m for 10min), they were subjected to hypotonic swelling (0.075M KCl (Sigma) at 37°C for 10-18min. Metaphase preparations were then fixed in ethanol: acetic acid (3:1 v/v) overnight at 4°C.

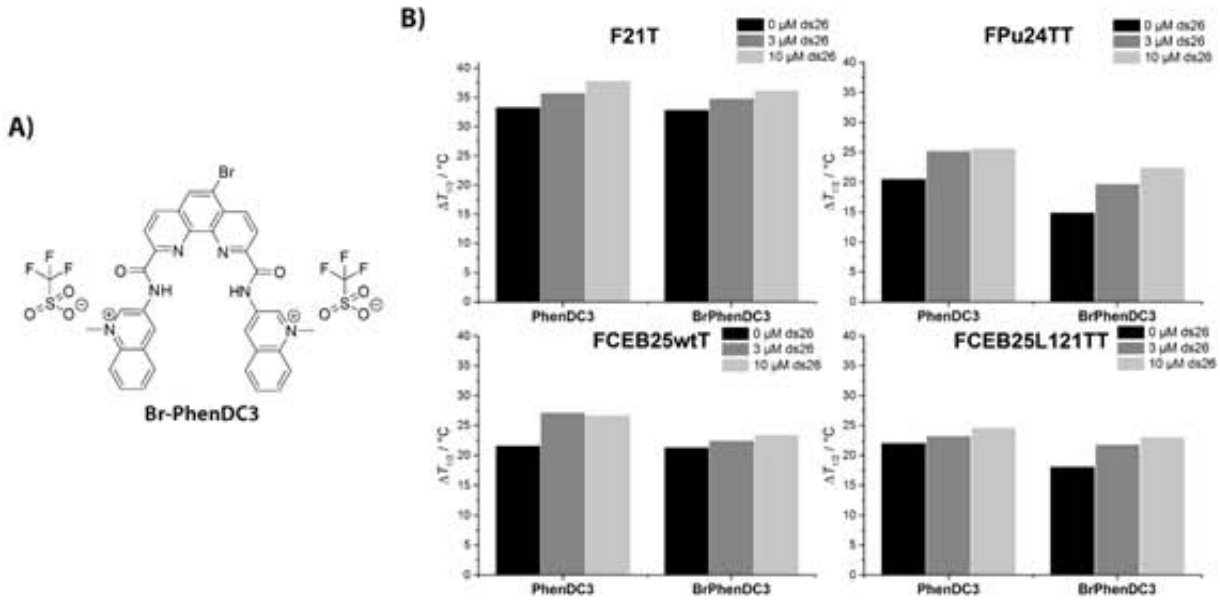

Figure 1: A) Br-PhenDC3 structure. B) Quantitative analysis of the FRET-melting competition experiments with the telomeric sequence (F21T), c-myc oncogene sequence (FPu24TT), mini satellite sequences FCEB25wtT and FCEB25L121TT. Stabilisation in: 10mM KCl + 90mM LiCl/10mM Lithium cacodylate pH 7.2 (F21T), or 1mM KCl + 99mM LiCl/10mM Lithium cacodylate pH 7.2 (FPu24TT, FCEB25wtT, and FCEB25L121TT) is shown for PhenDC3 used as a reference and Br-PhenDC3 in the absence (black bars) or presence of double-stranded DNA (ds26) at 3mm (dark grey bars) or 10mm (fair grey bars).

Percentage of cell growth inhibition

KB (keratin-forming tumor cell line HeLa), A549 (adenocarcinomic human alveolar basal epithelial cells), MCF7 (human breast adenocarcinoma cell line), MRC5 (human fetal lung fibroblast cells), HCT116 (human colon cancer cell line) cell lines were treated with various concentrations of Br-PhenDC3 and PhenDC3 at 37°C under humidity and 5% CO_2 conditions for 48 or 96h. Cellular growth was quantified using the particle counter Z2 Coulter® (Beckman, COULTER®).

NanoSIMS: sample preparation and imaging

HEK-293 metaphase chromosomes were spread onto silicon chip in the same manner as for preparation on glass slide for chromosome karyotype analysis. To reduce the hydrophobic property of bare silicon surface and to improve the chromosomes spreading, the surface of silicon chip was cleaned and activated by plasma (using a PELCO easiGlow, TED PELLA, INC). After drying in air, the silicon chip was introduced into a NanoSIMS-50 Ion microprobe (CAMECA, Gennevilliers, France) operating in scanning mode [24]. For the present study, by using a tightly focused Cs^+ primary ion beam, four secondary ion species ($^{12}C^-$, $^{12}C^{14}N^-$, $^{31}P^-$, as well as $^{81}Br^-$, an isotope with natural abundance of 49.3%) were monitored in parallel from the same sputtered volume. For the measurement of $^{81}Br^-$ signal, appropriate mass resolution was applied to prevent interference due to isobaric species. The primary beam steps over the surface of the sample to create images for these selected ion species. The primary beam intensity was 3pA with a typical probe size of ≈200nm. The raster size was from 50 to 60µm in order to image the whole karyotype from HEK-293 cell lines, with an image definition of 512 × 512 pixels. Due to the destructive nature of SIMS technique, in order to accumulate ion signal without damaging the chromosome structure, the image acquisition was carried out in multi-frame mode. With a dwell time of 0.5ms per pixel, up to 150 frames were acquired and the total analysis time was around 5h. Image processing was performed using the "ImageJ" software [25]. Successive image frames were properly aligned using TOMOJ plugin [26] with $^{12}C^{14}N^-$ images as reference before a summed image was obtained for each ion species.

Statistical analysis

Due to the low labeling level and despite the high detection efficiency, the counting rate (counts per second) for $^{81}Br^-$ ions under our experimental conditions is quite low. As the ion counting obeys the Poisson law, large counting fluctuation (uncertainty) is inevitable during NanoSIMS imaging. Therefore, long accumulation was performed in multi-frame mode. Then, by using a home-made ImageJ macro (supplementary material figure S2), average images from multi-frame acquisition was computed and only those pixels with averaged level higher than the maximum confidence interval value (p=0.9999) was retained as they are considered highly statistically significant. For each pixel, such maximum confidence interval value has been determined by adding to the averaged level, the Poisson law statistical error:

$$err = Z_{\alpha/2}\sqrt{\frac{\mu}{n}}$$

where $Z_{\alpha/2}$=3.72 (for α=0.0001), n is the number of averaged values and µ the average value computed for that pixel, respectively. Similar process has been performed for the P images.

In this way, the location of such highly significant $^{81}Br^-$ signal can be accurately determined which corresponds to the Br-PhenDC3 preferential binding sites. Furthermore, this allows us to compute the pixel intensity profiles of chromatids alone each chromosome on the Br-significant images in order to determine if chromosomal domains are Br-PhenDC3 labelled. On these profiles the Spearman correlation

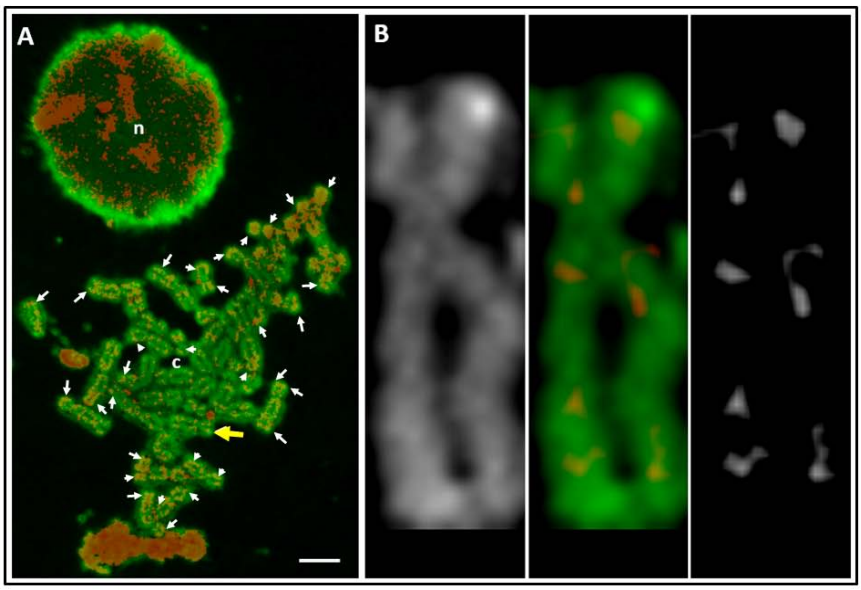

Figure 2: NanoSIMS analysis. A) Overlay of significant (p=0.9999) Br (red) and P (green) NanoSIMS images depicting the localization of Br in discrete regions in chromosomes center, c) and nucleus (top, n).White arrows point some telomere regions on chromosomes. Scale bar 4µm. B) Numerical zoom of single chromosome indicated by yellow arrow in (A). Left P signal; Middle, overlay of Br (red) and P (green) signals; right Br significant (p=0.9999) signal.

coefficients were determined using the Excel functionsRANK.AVG followed by CORREL and the positions of the maxima were visually compared. The p-values were computed in Excel using T.DIST.2T for each Spearman correlation coefficient.

Results and Discussion

In vitro evaluation was performed by classical FRET-melting assay in the presence of well-known G-quadruplex sequences, such as the human telomeric sequence (F21T), the c-myc oncogene sequence (FPu24TT), and the mini-satellite sequences FCEB25wtT and FCEB25L121TT. The data on Figure 1 indicate that Br-PhenDC3 retains the affinity of PhenDC3as variation in melting temperature induced by the ligand on the four G4 matrices (ΔTm) have very close values: ΔTm (PhenDC3) *vs* ΔTm (Br-PhenDC3): F21T =33 °C*vs* 32°C, FPu24TT=20°C*vs* 15°C, FCEB25wtT = 22°C*vs*21 and FCEB25L121TT =22°C *vs* 18°C. As well the binding of Br-PhenDC3 is not significantly modified in presence of the duplex competitor ds26 (Figure 1, grey bars), thereby revealing a high selectivity for G4 structures. *In cellulo* Br-PhenDC3 exhibits moderate cytoxicity close to that of PhenDC3as evaluated on a large panel of human cancer cell lines (KB, A549, MCF7, MRC5, and HCT116, Table S1). Altogether these data indicate that the addition of a bromine atom on PhenDC3 has no or poor effect on the *in vitro* affinity and selectivity for the G4 targets and on the *in cellulo* activity as compared to the non labelled compound. These results make possible to assume that the two compounds have similar behavior in cells and that their genomic distribution should be similar, which confirms that the brominated derivative can be used reliably to locate G4 structures.

The analysis of statistically significant $^{81}Br^-$ images was then performed on samples containing both entire nuclei and metaphase chromosomes isolated from cells incubated with a subtoxic dose (0.3µM) of Br-PhenDC3. The merge of $^{81}Br^-$images with the $^{31}P^-$ map typical of DNA allows evaluating the genomic distribution of the compound (Figure 2, Figure S3). First examination indicates a non-homogeneous distribution of the ligand at the level of nucleus (Figure 2A) which evidences binding in specific regions as expected from the ligand preference for non-canonical DNA structures. Secondly, observation of chromosome spread shows that the molecule is located to telomeric regions on almost all chromosomes (Figure 2A and S3). Finally, in addition to the telomeric localization of Br-PhenDC3, the reliable NanoSIMS images allow us to observe Br-PhenDC3 labelling in non-telomeric domains which may vary significantly from one chromosome to another(Figure 2 and S3). Remarkably the sensitivity in detecting Br-labelled molecules and the high spatial resolution provided by NanoSIMS permit not only to locate Br-PhenDC3 in various non-telomeric regions but also to precisely determine its position in each chromatid of a chromosome (Figure S3B). Supplementary Figure S3 illustrates that it is possible to take advantage of this approach to study if Br-PhenDC3 binds in specific domains of chromatids. Effectively, in case of the existence of specific G4 domains in chromosomes, the $^{81}Br^-$signal should be placed at equivalent positions in each chromatid. This is easy to verify by plotting the integrated pixel intensity profile of the $^{81}Br^-$ signal from each chromatid computed by adding pixel values along the chromatid axis and comparing the two plots (Figure S3). The analysis of 5 chromosomes, depicted as an example on supplementary Figure S3A, shows that the position of most of the Br-peaks overlap, or are close, in sister chromatids. Moreover, the Spearman correlation coefficients (-0.0505, 0.6814, 0.5808, 0.5455 and 0.6278) show a significant correlation of four over five chromosomes analyzed (p-values 0.55, <0.0001, <0.0001, <0.0001, <0.0001 respectively) (Figure S3B). In the case where the correlation is not significant this can be explained by two effects: shifts in the positions of the maxima and absence of some peaks. The shifts can be explained by the fact that chromatid fibers are not straight and parallel and might be coiled to a certain extent. The absence can be justified by unspecific binding of Br-PhenDC3

to regions in which G4 structures are not present. Therefore, we can consider that Br-PhenDC3 binding is not random as it occurs mainly at the same position in the two sister chromatids of all the chromosomes analyzed.

Few methods have been reported to visualize G4 ligands on metaphase chromosomes which suffer from intrinsic limitations. So far the only example of direct localisation of G4 ligand on chromosomes has been provided by Boussin et al. [27] in a pioneering study in which a tritium (^{3}H) radiolabeled derivative of the bisquinolinium drug PDC (360A) was used to evaluate its distribution on metaphase human chromosomes. The drug localization was observed both in terminal and interstitial chromosome regions in consistency with our study. However, this method requires the use of radioisotopes and the obtained spatial resolution cannot rival the one achieved in the present study by NanoSIMS. The presence of a fluorescent G4-ligand (BMVC) at telomeric extremities of chromosomes has also been observed using Fluorescence Lifetime IMaging (FLIM) [28,29], but with low accuracy and poor spatial resolution compared to those obtained by NanoSIMS imaging. A more recent study reveals that FLIM might be a powerful method for mapping G4 in cells using the fluorescent probe DOTA but seems so far more adapted to nuclear DNA imaging [30]. Finally fluorescent immunostaining with multiply labeled G4-antibodieshas enabled the detection of large fluorescent G4-foci located in telomeric (25%) and other regions (75%) of chromosomes but still with intrinsically limited resolution [31]. Altogether our data are fully consistent with the G4 localization approaches reported so far, which make use of either G4 interactive compounds or G4-antibodies, with the outstanding difference that the precision and spatial resolution proposed herein are unprecedented.

Finally, a complementary approach to get more information on the ligand distribution observed in our study in correlation with the presence of G4 domains would be to perform karyotype analysis of the sample in the aim evaluating if there is specific enrichment of the signal for chromosomes that are known to contain G-rich domains (comparison of chromosomes 17 and 19 for instance). The quality of the sample did not allow complete karyotyping, but a partial analysis could be done resulting in identification of six pairs of chromosomes (data not shown), which emphasizes the powerfulness of the proposed method and validates this imaging combined approach.

Conclusion

We applied NanoSIMS imaging for mapping the distribution of the bromo-labelled G4 ligand PhenDC3 on metaphase human chromosomes. We showed that the ligand localizes both at terminal and interstitial regions with a high spatial resolution surpassing that of all other methods reported so far. The distribution may vary from one chromosome to another but is globally similar on sister chromatids, which is fully consistent with the presence of specific DNA domains bound by the G4 drug. To fully strengthen our approach complementary experiments in various cellular contexts and with different drug isotopic label signatures will be performed in the future. Nonetheless our study already represents the first step towards genome-wide mapping of DNA interactive drugs using chromosome chemical imaging that is both alternative and fully complementary to other existing approaches.

Acknowledgement

Authors want to thanks the PICT-IBiSA for providing access to chemical imaging facility.

Supplementary Material

http://austinpublishinggroup.com/molecular-biology/fulltext/Sup-jmbmi-v4-id1029.docx

References

1. Anders L, Guenther MG, Qi J, Fan ZP, Marineau JJ, Rahl PB, et al. Genome-wide localization of small molecules. Nature Biotech. 2014; 32: 92-96.
2. Müller S, Kumari S, Rodriguez R, Balasubramanian S. Small-molecule-mediated G-quadruplex isolation from human cells. Nat. Chem. 2010; 2: 1095-1098.
3. Shu X, Xiong X, Song J, He C, Yi C. Base-Resolution Analysis of Cisplatin-DNA Adducts at the Genome Scale. Angewandte Chemie Int Ed. 2016; 55: 14246-14249.
4. Hua J, Liebb JD, Sancara A, Adara S. Cisplatin DNA damage and repair maps of the human genome at single-nucleotide resolution. Proc. Natl. Acad. Sci. USA. 2016; 113: 11507-11512.
5. Meier JL, Yu AS, Korf I, Segal DJ, Dervan PB. Guiding the design of synthetic DNA-binding molecules with massively parallel sequencing. J. Am. Chem. Soc. 2012; 134: 17814–17822.
6. Anandhakumar C, Li Y, Kizaki S, Pandian GN, Hashiya K, Bando T, et al. Next-generation sequencing studies guide the design of pyrrole-imidazole polyamides with improved binding specificity by the addition of β-alanine. Chembiochem. 2014; 15: 2647-2651.
7. Moore I, Murphy A. Validating the location of fluorescent protein fusions in the endomembrane system. Plant Cell. 2009; 21: 1632-1636.
8. Millar AH, Carrie C, Pogson B, Whelan J. Exploring the function-location nexus: Using multiple lines of evidence in defining the subcellular location of plant proteins. Plant Cell. 2009; 21: 1625–1631.
9. Hanson DA, Ziegler SF. Fusion of green fluorescent protein to the C-terminus of granulysin alters its intracellular localization in comparison to the native molecule. J Negat Results Biomed. 2004; 3: 2.
10. Lipps HJ, Rhodes D. G-quadruplex structures: *in vivo* evidence and function. Trends Cell Biol. 2009; 19: 414-422.
11. Balasubramanian S, Hurley LH, Neidle S. Targeting G-quadruplexes in gene promoters: a novel anticancer strategy? Nature drug discov. 2011; 10: 261-275.
12. Zimmer J, Tacconi EM, Folio C, Badie S, Porru M, Klare K, et al. Targeting BRCA1 and BRCA2 Deficiencies with G-Quadruplex-Interacting Compounds. Mol. Cell. 2016; 61: 449-460.
13. Merle P, Gueugneau M, Teulade-Fichou MP, Müller-Barthélémy M, Amiard S, Chautard E, et al. Highly efficient radiosensitization of human glioblastoma and lung cancer cells by a G-quadruplex DNA binding compound. Sci. Reports. 2015; 5: 16255.
14. Ohnmacht SA, Neidle S. Small-molecule quadruplex-targeted drug discovery. Bioorg Med Chem Lett. 2014; 24: 2602-2612.
15. Müller S, Rodriguez R. G-quadruplex interacting small molecules and drugs: from bench toward bedside. Expert Rev. Clin. Pharmacol. 2014; 7: 663-679.
16. Cogoi S, Xodo LE. G4 DNA in ras genes and its potential in cancer therapy. Biochim. Biophys. Acta. 2016; 1859: 663-674.
17. Jun Chung W, Heddi B, Hamon F, Teulade-Fichou MP, Phan AT. Solution structure of a G-quadruplex bound to the bisquinolinium compound Phen-DC3. Angew. Chem. Int. Ed. 2014; 53: 999 -1002.
18. Piazza A, Boule JB, Lopes J, Mingo K, Largy E, Teulade-Fichou MP, et al. Genetic instability triggered by G-quadruplex interacting Phen-DC compounds in Saccharomyces cerevisiae. Nucleic Acids Research, 2010; 38: 4337-4348.

19. Piazza A, Adrian M, Samazan F, Heddi B, Hamon F, Serero A, et al. Short loop length and high thermal stability determine genomic instability induced by G-quadruplex-forming minisatellites. EMBO J. 2015; 34: 1718-1734.

20. Lopes J, Piazza A, Bermejo R, Kriegsman B, Colosio A, Teulade-Fichou MP, et al. G-quadruplex-induced instability during leading-strand replication. EMBO J. 2011; 30: 4033-4046.

21. Guerquin-Kern JL, Wu TD, Quintana C, Croisy A. Progress in analytical imaging of the cell by dynamic secondary ion mass spectrometry (SIMS microscopy). Biochimica et Biophysica Acta. 2005; 1724: 228–238.

22. Lechene C, Hillion F, McMahon G, Benson D, Kleinfeld AM, Kampf JP, et al. High-resolution quantitative imaging of mammalian and bacterial cells using stable isotope mass spectrometry. Journal of Biology. 2006; 5: 20.

23. Howe B, Umrigar A, Tsien F. Chromosome preparation from cultured cells. J Vis Exp. 2014; 83: e50203.

24. Guerquin-Kern JL, Hillion F, Madelmont JC, Labarre P, Papon J, Croisy A. Ultra-structural cell distribution of the melanoma marker iodobenzamide: improved potentiality of SIMS imaging in life sciences. Biomed. Eng. 2004; 3: 10.

25. Schneider CA, Rasband WS, Eliceiri KW. NIH Image to ImageJ: 25 years of image analysis. Nat Methods. 2012; 9: 671-675.

26. Messaoudi C, Boudier T, Sanchez Sorzano CO, Marco S. TomoJ: tomography software for three-dimensional reconstruction in transmission electron microscopy. BMC bioinformatics. 2007; 8: 288.

27. Granotier C, Pennarun G, Riou L, Hoffschir F, Gauthier LR, De Cian A, et al. Preferential binding of a G-quadruplex ligand to human chromosome ends. Nucleic Acids Res. 2005; 33: 4182-4190.

28. Chang CC, Chu JF, Kao FJ, Chiu YC, Lou PJ, Chen HC, et al. Verification of antiparallel G-quadruplex structure in human telomeres by using two-photon excitation fluorescence lifetime imaging microscopy of the 3,6-Bis(1-methyl-4-vinylpyridinium)carbazole diiodide molecule. Anal. Chem. 2006; 78: 2810-2815.

29. Largy E, Granzhan A, Hamon F, Verga D, Teulade-Fichou MP. Visualizing the quadruplex: from fluorescent ligands to light-up probes. Top. Curr. Chem. 2013; 330: 111-177.

30. Shivalingam A, Izquierdo MA, Marois AL, Vyšniauskas A, Suhling K, Kuimova MK, et al. The interactions between a small molecule and G-quadruplexes are visualized by fluorescence lifetime imaging microscopy. Nat. Commun. 2015; 6: 8178.

31. Biffi G, Tannahill D, McCafferty J, Balasubramanian S. Quantitative visualization of DNA G-quadruplex structures in human cells. Nat. Chem. 2013; 5: 182-186.

J Mol Biol & Mol Imaging - Volume 4 Issue 1 - 2017
ISSN : 2471-0237 | www.austinpublishinggroup.com

Citation: Verga D, Hamon F, Nicoleau C, Guetta C, Wu TD, Guerquin-Kern JL, et al. Chemical Imaging by NanoSIMS Provides High-Resolution Localization of the G-Quadruplex Interactive Drug (Br)-PhenDC3 on Human Chromosomes. J Mol Biol & Mol Imaging. 2017; 4(1): 1029.